Journal of Theoretical Biology 332 (2013) 30–41

Contents lists available at SciVerse ScienceDirect

Journal of Theoretical Biology

journal homepage: www.elsevier.com/locate/yjtbi

The role of the bacterial mismatch repair system in SOS-induced mutagenesis: A theoretical background

Oleg V. Belov [a,*], Ochbadrakh Chuluunbaatar [b,c], Mikhail I. Kapralov [a], Nasser H. Sweilam [d]

[a] Laboratory of Radiation Biology, Joint Institute for Nuclear Research, 6 Joliot–Curie Street, 141980 Dubna, Moscow Region, Russia
[b] Laboratory of Information Technologies, Joint Institute for Nuclear Research, 6 Joliot–Curie Street, 141980 Dubna, Moscow Region, Russia
[c] School of Mathematics and Computer Science, National University of Mongolia, 1 Central Ulaanbaatar, PO Box 46a/523, 210646, Mongolia
[d] Mathematics Department, Faculty of Science, Cairo University, Giza 12613, Egypt

HIGHLIGHTS

- A mathematical model of the bacterial DNA mismatch repair system is developed.
- Five key pathways of the *Escherichia coli* mismatch repair are simulated adequately.
- The relationships between SOS and MMR systems are described quantitatively.
- A possible mechanistic explanation of MMR role in UV-mutagenesis is shown.

ARTICLE INFO

Article history:
Received 29 August 2012
Received in revised form
20 April 2013
Accepted 22 April 2013
Available online 30 April 2013

Keywords:
SOS response
Mismatch repair
UV mutagenesis
Mathematical modeling

ABSTRACT

A theoretical study is performed of the possible role of the methyl-directed mismatch repair system in the ultraviolet-induced mutagenesis of *Escherichia coli* bacterial cells. For this purpose, mathematical models of the SOS network, translesion synthesis and mismatch repair are developed. Within the proposed models, the key pathways of these repair systems were simulated on the basis of modern experimental data related to their mechanisms. Our model approach shows a possible mechanistic explanation of the hypothesis that the bacterial mismatch repair system is responsible for attenuation of mutation frequency during ultraviolet-induced SOS response via removal of the nucleotides misincorporated by DNA polymerase V (the UmuD'$_2$C complex).

1. Introduction

One of the biological systems capable of correcting the non-complementary nucleotide pairs that appear as a consequence of certain factors is the methyl-directed mismatch repair system (MMR) (Lahue et al., 1989; Modrich and Lahue, 1996). The evidences of the functioning of this system were found in many organisms including bacteria, yeasts, and mammals. Despite high MMR conservability and the similarity of the repair mechanisms between bacteria and mammals, the interrelations of its pathways and other repair systems are well understood only for relatively simple biological objects like prokaryotic cells.

The factors which can start the MMR system may include the errors that occur during normal DNA replication and cell metabolism as well as a spectrum of DNA lesions induced by exposure to different agents of physical and chemical nature and the following DNA repair processes (Li, 2008). Among the physical factors capable of inducing this system, the action of radiations of different types is very interesting in terms of its use as an instrument for studying the MMR connections with other repair systems responsible for the mutagenic effects in the living organisms. A number of experimental facts indicate that MMR plays a certain role in the mutagenic effects of ionizing and ultraviolet (UV) radiation (Hongbo et al., 2000; Martin et al., 2010). Some of these facts suggest the involvement of MMR in mutagenic pathways of other repair systems.

Among the pathways leading to an increase in the mutation frequency and other negative effects under the influence of physical and chemical factors, an important role belongs to the SOS repair system (Radman, 1974; Witkin, 1976; Krasavin and Kozubek, 1991). Intense studies of the SOS response of prokaryotic cells have identified the key role of the specific PolV Mut complex comprising DNA polymerase V (or UmuD'$_2$C) in the process of DNA

* Corresponding author. Tel.: +7 49621 62847; fax: +7 49621 65948.
E-mail addresses: dem@jinr.ru (O.V. Belov), chuka@jinr.ru (O. Chuluunbaatar), nsweilam@sci.cu.edu.eg (N.H. Sweilam).

0022-5193/$ - see front matter © 2013 Elsevier Ltd. All rights reserved.
http://dx.doi.org/10.1016/j.jtbi.2013.04.026

synthesis through the lesion which was called translesion synthesis (TLS) (Wang, 2001). This mechanism is also realized not only in prokaryotic cells but in mammalian and human cells, too (Yang et al., 2003; Chiapperino et al., 2005).

Experimental studies have shown that PolV Mut demonstrates a relatively high error frequency during the incorporation of bases in nascent strands opposite the lesions which were not removed during the earlier stages of repair (Tang et al., 2000). However, the finally measured mutation frequency in individual genes is not so high as it might have been if all mismatches produced by the PolV Mut complex had been fixed as mutations. Our previous research related to the mathematical modeling of the mechanism of SOS-induced mutagenesis under 254 nm ultraviolet (UV) radiation demonstrated this fact by an interval of the free parameter value responsible for fixing the PolV-induced mismatches as mutations (Belov et al., 2009). These conclusions made us introduce in our model additional repair mechanisms at the final stages of SOS response. Taking into account the specific character of DNA synthesis by the PolV Mut complex and relying on the corresponding experimental facts, we have chosen the MMR system of *Escherichia coli* bacterial cells for the theoretical analysis of its influence on the UV-induced mutagenic effect. So, the main goal of this study is to identify the role of MMR in SOS-induced mutagenesis on the basis of the precise modeling of the enzymatic mechanisms of these two repair systems under exposure to radiation.

2. Mathematical model

2.1. A quantitative model of the SOS network

UV radiation induces two major types of photoadducts in DNA, namely, thymine–thymine cys–syn cyclobutane photodimers and thymine–thymine pyrimidine (6–4) pyrimidone photoproducts. A significant portion of the primary induced thymine dimers are efficiently removed by pre-replication mechanisms such as phtotoreactivation (Rupert, 1975) and nucleotide excision repair (NER) (Sancar and Sancar, 1988). The lesions which were not removed by these repair mechanisms lead to the production of single-stranded DNA gaps (ssDNA) in bacterial chromosomes that prevent successful replication completion (Rupp and Howard-Flanders, 1968). To process the remaining single-stranded gaps, cells actuate a number of specific repair mechanisms called SOS response (Radman, 1974). Therefore, ssDNA is regarded as an inducing signal for a cell to launch the SOS system.

To describe the dynamics of SOS signal induction, we used the mathematical approach developed earlier (Belov et al., 2009; Aksenov, 1999). The final dimensionless equations of this model are as follows:

$$\begin{aligned} &\text{for} \quad \tau < \tau_2 \; x_0(\tau,\Psi) = \Psi \exp(-q_1\tau) \int_0^{\tau} \frac{\exp(q_1\xi)d\xi}{q_2\Psi+\exp(q_3\xi)}, \\ &\text{for} \quad \tau \geq \tau_2 \; x_0(\tau,\Psi) = \Psi \exp(-q_1\tau) \int_0^{\tau_2} \frac{\exp(q_1\xi)d\xi}{q_2\Psi+\exp(q_3\xi)}, \end{aligned} \tag{1}$$

where

$$\tau_2 = \frac{1}{q_3}\ln(\exp(q_4)(1+q_2\Psi)-q_2\Psi).$$

Here, x_0 is the normalized intracellular concentration of ssDNA, Ψ is the UV energy fluence, τ is the dimensionless time, τ_2 is the dimensionless time of replication termination, ξ is the integration variable, and q_i ($i=1,\ldots,4$) are the dimensionless kinetic parameters of the model (see Appendix A).

Since most of the experiments on UV-induced mutagenesis are carried out in dark conditions, the influence of photoreactivation is excluded in this model. The source of the SOS-inducing signal is represented here as a superposition of two processes, namely, DNA replication and NER. The dynamics of ssDNA induction is determined on the basis of the balance between the five fractions of DNA disorders appearing in the bacterial chromosome after UV irradiation. They include the dimers initially produced by UV, the gaps opposite dimers, the dimers located in front of the replisome, the dimers removed by NER in front of the replisome, and the repaired gaps. This approach takes into account the facts that NER is pre-replication repair and its ferments operate in front of the replisome in the chromosome. The inducing signal is determined as the ss-gaps located opposite thymine dimers not removed by NER and formed as a consequence of replication restart beyond a dimer. DNA replication and dimer removal are regarded as parallel processes where NER leads. Therefore, the inducing signal terminates together with replication. The ssDNA sequences generated at any later stage of repair machinery are not considered as a contribution to the inducing signal for SOS response. Since NER cuts UV-generated dimers, it significantly reduces the number of primary DNA lesions. Thus, NER directly contributes to the total pool of SOS signal and indirectly impacts the number of mismatches and finally produced mutations.

The model assumptions mentioned above imply introducing the replication termination time, which depends on the number of produced dimers and, consequently, on UV energy fluence. Therefore, if the computation interval is less than the time of replication termination, the model of inducing signal should be calculated until the end of the stated interval. Otherwise, a calculation should be done until the replication time termination because after that, the inducing signal cannot be generated.

Further steps of SOS system functioning are connected with the activity of more than 40 genes controlled by LexA repressor. In our model, we consider four of these genes which make a major contribution to the regulation of the bacterial SOS function. They are the *recA*, *lexA*, *umuD*, and *umuC* genes. After ssDNA has been produced, the product of the *recA* gene binds to it and transforms into the active RecA* form. The activated RecA protein has a specific protease conformation, which makes it able to cleave the LexA repressor as well as a number of other proteins. A decrease in the LexA protein level leads to the enhanced expression of the repressed genes including *recA*, *lexA*, *umuD*, and *umuC*. Despite an increase in *lexA* gene expression, it does not lead to raising the level of LexA protein due to its immediate cleavage by RecA* (Krasavin and Kozubek, 1991). The RecA protease also cleaves the UmuD protein, transforming it into the UmuD' active form. The normal and active forms of the UmuD protein can form dimers of three types, namely, $UmuD_2$, UmuDD', and $UmuD'_2$ (Burckhardt et al., 1988; Woodgate et al., 1989). These dimers are able to interact with UmuC, forming $UmuD_2C$, UmuDD'C, and $UmuD'_2C$ complexes, respectively.

The main role in an induced mutation process in *E. coli* belongs to $UmuD'_2C$ (or DNA polymerase V, PolV). This protein complex is able to form a multienzyme complex called PolV Mut, which includes molecules of the RecA-protease, SSB-proteins, and subunits of DNA polymerase III. The PolV Mut complex is able to fill the remaining single-stranded gaps by inserting nucleotides in a random manner. This allows a chromosome to be fully replicated. However, the daughter DNA sequence contains defects due to the specificity of PolV Mut-mediated gap filling.

The $UmuD_2C$ and UmuDD'C complexes play a supplementary role in the SOS function. $UmuD_2C$ is involved in cell cycle regulation. It stops replicative DNA synthesis and allows the TLS process to be realized in the presence of SOS-inducing damage. The UmuDD'C has an inhibiting function in SOS mutagenesis that consists in suppressing the UmuD' activity (Smith and Walker, 1998).

To simulate the above-mentioned stages of SOS repair, we used a quantitative model proposed earlier (Belov et al., 2009). The

dynamic change of the concentration of the main SOS proteins is expressed in general by the following differential equations:

$$\frac{dX}{dt} = V_+(X_i, X_0) - V_-(X_i, X_0), \tag{2}$$

where X_i $(i = 1, \ldots\ldots n)$ is the i-th regulatory protein intracellular concentration, X_0 is the level of an inducing signal (ssDNA), t is time, V_+ is the regulatory protein synthesis rate, and V_- is the regulatory protein degradation rate. The functions V_+ and V_- describe the protein accumulation and degradation, respectively. The equations reflecting the dynamic change of each SOS protein's concentration as well as the estimation of their parameters and initial conditions are presented in the respective subsections of Appendix A.

2.2. A model of translesion synthesis

To describe the induction of mismatches during SOS repair, we have used a translesion synthesis model published earlier (Belov et al., 2009). When we analyze the probability of errors appearing during TLS we need to model a random quantity which is the number of mismatches in DNA chain. These mismatches appear during fixed time under the assumption that all these events are independent and occur with some average fixed intensity. Since the number of nucleotides n supplied by PolV Mut is large (about several thousand) and a mutation probability in each individual nucleotide pasting is low (about 10^{-4}–10^{-3} (Tang et al., 2000)) we can conclude that the number of mismatches m appearing in DNA chain is distributed by Poisson's law:

$$P_n(m) = \frac{a^m}{m!} e^{-a}.$$

The calculation of the Poisson distribution parameter a is performed using a special code developed earlier (Belov et al., 2009). The code models PolV Mut moving along DNA and finds a fluence-time dependence of the parameter a using the fluence-time dependence of the PolV complex, which is characterized by the variable x_{11} from Eq. (A.1) (see Appendix A). Here we put the number of PolV Mut molecules equal to the number of PolV molecules because it is known that only one PolV molecules participate in the resynthesis of each ssDNA site (Pham et al., 2001). In this research, we also consider the possibility of PolV Mut involvement in the replication of ssDNA sites which do not contain thymine dimers. This assumption is based on the fact that PolV Mut can realize TLS at undamaged DNA (Tang et al., 2000). In our model, we separate the replication processes realized directly at the thymine dimers, at the rest of the ssDNA gaps without dimers, and at the other undamaged ssDNA sites contained in the cell at this moment. The developed code models the occurrence of nucleotide mismatches during TLS taking into account the individual peculiarities and characteristics of all three processes.

The replication at the thymine dimers described as a step-by-step calculation of number $L_{td}(\tau, \Psi)$ of nucleotides inserted by PolV Mut. The formula for calculation is

$$L_{td}(\tau, \Psi) = x_{11}(\tau, \Psi) v_{td}\left(\tau - \tau_{in} + \frac{l_1}{2\, v_{ss}}\right) \tag{3}$$

In Eq. (3), the number of the PolV Mut molecules is equal to the number of the DNA PolV molecules $x_{11}(\tau, \Psi)$. ν_{td} is the velocity of PolV Mut moving at the moment when it passes thymine dimers, τ_{in} is the normalized time when the last of the $x_{11}(\tau, \Psi)$ PolV molecules present at this moment was synthesized. The calculation of v_{td} is based on the data on the average length of the ssDNA gap l_1 and the termination time of the whole TLS process for a specific UV energy fluence. v_{ss} is the velocity of PolV Mut movement during the filling of the ssDNA sites.

The replication at the single-stranded DNA gaps excluding thymine dimers is described by the formula

$$\left[\begin{array}{l} \begin{cases} L_{ss}(\tau, \Psi) = x_{11}(\tau, \Psi) v_{ss}(\tau - \tau_{in}), \\ x_{11}(\tau, \Psi) \le N_1(\Psi), \end{cases} \\ \begin{cases} L_{ss}(\tau, \Psi) = N_1(\Psi) v_{ss}(\tau - \tau_{in}), \\ x_{11}(\tau, \Psi) > N_1(\Psi), \end{cases} \end{array}\right. \tag{4}$$

where $L_{ss}(\tau, \Psi)$ is number of nucleotides supplied by PolV Mut at current moment, $N_1(\Psi)$ is the number of ssDNA gaps formed till the replication termination. $N_1(\Psi)$ was calculated as in detail described by Aksenov (1999) and Aksenov et al. (1997).

PolV Mut-mediated replication at undamaged ssDNA is described using the following approach. Since the PolV Mut complex has a great affinity to single DNA associated with the RecA protein, it can be concluded that the TLS begins and ends at ssDNA gaps. Consequently, the inclusion of PolV Mut in the process at the undamaged DNA occurs at a time when its number becomes to exceed the number of single-stranded gaps produced by nucleotide excision repair. Accordingly, the termination of synthesis on undamaged DNA occurs at a time when the number of molecules of PolV Mut becomes equal to the number of single spaces. Sequential calculation of the number $L_{und}(\tau, \Psi)$ of supplied nucleotides in this case is described by the formula

$$\left[\begin{array}{l} \begin{cases} L_{und}(\tau, \Psi) = 0, \\ x_{11}(\tau, \Psi) \le N_1(\Psi), \end{cases} \\ \begin{cases} L_{und}(\tau, \Psi) = v_{ss}(x_{11}(\tau, \Psi) - N_1(\Psi), \\ x_{11}(\tau, \Psi) > N_1(\Psi). \end{cases} \end{array}\right. \tag{5}$$

The fluence-time dependence for the parameter a is calculated in our code by the following formula:

$$a(\tau, \Psi) = P_{ss}(L_{und}(\tau, \Psi) + L_{ss}(\tau, \Psi)) + P_{td} L_{td}(\tau, \Psi), \tag{6}$$

where P_{ss} is a probability of mismatch induction during nucleotide pasting by PolV Mut on DNA sites which do not contain thymine dimers; P_{td} is the mismatch induction probability during thymine dimer processing. The probability P_{td} was calculated as follows:

$$P_{td} = P_1 P_A + P_2 P_B + P_3 P_C + P_4 P_D, \tag{7}$$

where P_A, P_B, P_C, and P_D are the probabilities of a single mismatch occurrence during processing TT (6–4) photoproduct with a 3'-end, TT (6–4) photoproduct with a 5'-end, cys–syn cyclobutane photodimer with a 3'-end, and cys–syn cyclobutane photodimer with a 5'-end, respectively. P_1, P_2, P_3, and P_4 are the probabilities of generating each of the four types of lesions. Estimation of the TLS model parameters is presented in Appendix A.

In our model, the variable $a(\tau, \Psi)$ calculated by formula (6) is the parameter through which the PolV concentration contributes first to the mismatch induction, and then to the mutation rate.

2.3. A model of DNA mismatch repair

Following the induction of SOS response, the frequency of misincorporated bases that are the substrate for MMR increases as compared to normal conditions. Recently a number of experimental observations led to the hypothesis that the MMR system significantly reduces the error rates during DNA replication by recognizing and correcting mismatches which prevent normal replication (Kornberg and Baker, 1992). It was also found that MMR can process the incorrect bases opposite UV-induced photoproducts which were not removed by early repair processes like photoreactivation or nucleotide excision repair and during SOS response (Hongbo et al., 2000). Summarizing all these findings, we consider the methyl-directed excision of incorrect bases inserted

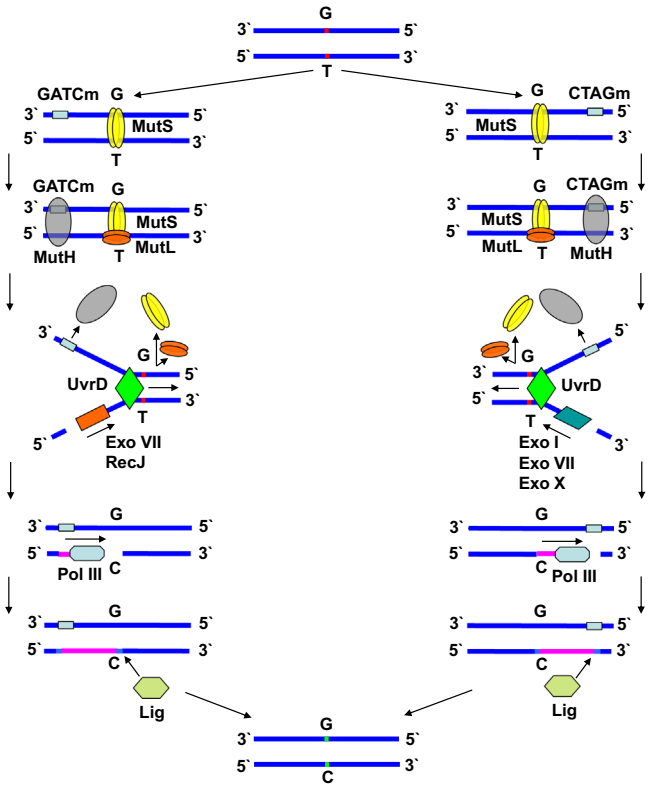

Fig. 1. Scheme of the MMR mechanism in *E. coli* bacterial cells (explanation in text).

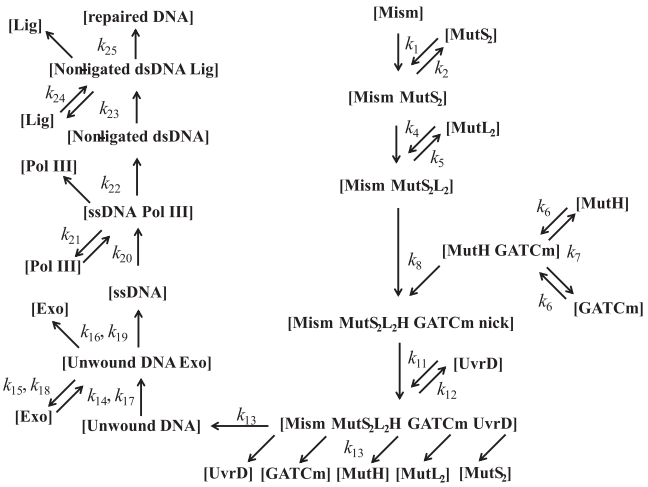

Fig. 2. Scheme representing the MMR reaction network used in the model. The synthesis and nonspecific losses of the MMR proteins are omitted.

by PolV Mut to be the main pathway of the interaction between the SOS system and MMR.

To describe the relationship between these systems we have developed a quantitative model of MMR which assumes the following molecular mechanism generalized as a scheme in Fig. 1. After the appearance of misincorporated nucleotides in the DNA chain, *E. coli*'s MMR system detects the mismatch shortly after the DNA replication round ends. The way to detect an incorrect base on the newly synthetized strand is based on the process of DNA methylation, which does not occur until several minutes after the strand is produced. This mechanism provides a distinction between the parental strand, which is already methylated, and the daughter strand containing an error (Lahue et al., 1989; Radman and Wagner, 1986). The recognition of a wrongly incorporated nucleotide is performed by the MutS protein, which binds to the site with a mismatch as a homodimer and forms a complex with the MutL protein. Interaction with MutL enhances mismatch recognition, and recruits MutH protein to the region. MutL also functions as a homodimer—in contrast with MutH, which acts as a monomer (Li, 2008). MutH finds a hemimethylated dGATC sequence and joins the unmethylated DNA strand. Then the $MutS_2L_2$ complex activates the MutH protein in the presence of ATP. During this interaction, MutH makes a strand-specific nick that can occur either 3' or 5' to the mispair on the unmethylated strand. Since the incision can be initiated on either 3' or 5' side of the mismatch, the MMR system is regarded as bidirectional process. In the presence of MutL, helicase II (or UvrD) loads at the nicked site and unwinds the nascent strand (Matson and Robertson, 2006). The single-stranded DNA (ssDNA) produced in this process is bound by the single-strand binding protein (SSB), which protects ssDNA from a nuclease attack. Further MMR steps require the activity of four exonucleases: ExoI, ExoVII, ExoX, and RecJ encoded by the *xonA*, *xseA*, *exoX*, and *recJ* genes, respectively. These exonucleases are able to digest the nonmethylated strand from the dGATC nicked site to just beyond the mismatch. The MMR exonucleases could proceed from 5' to 3' or from 3' to 5' end to the mispair (Li, 2008). ExoI and ExoX digest the DNA strand in the 3' to 5' direction, RecJ degrades it from 5' to 3', and ExoVII can excise DNA in both directions (Dutra et al., 2007). The resulting single-stranded gap is filled by DNA polymerase III holoenzyme (PolIII) with SSB. The remaining DNA strand is joined to existing one by the DNA ligase (Modrich and Lahue, 1996). The reaction network, which highlights mass transfer and regulatory reactions, is presented in Fig. 2.

To simulate the dynamic changes of the MMR protein levels, we used reversible mass-action kinetics based on Eq. (2). We singled out two MMR pathways with different exonucleases possessing polarity 3' or 5'. The dimensionless equations for each protein and intermediate complexes of the MMR system are given in Appendix B (Eq. B.1). In this study, we assume that 3' and 5' MutH-mediated nicks as well as the involvement of exonucleases possessing the same end specificity are equally probable. We also take into account the fact that none of the MMR enzymes except UvrD are controlled by the SOS system, i.e. their synthesis is not controlled by the LexA protein. However the expression of the *uvrD* gene producing helicase II depends on the intracellular concentration of the LexA repressor (Easton and Kushner, 1983; Courcelle et al., 2001). To describe the regulation of the *uvrD* transcription by the LexA protein, we used the model of gene regulation used in many papers (Belov et al., 2009; Aksenov et al., 1997; Aksenov, 1999). The first term in the equation for the UvrD helicase (y_9 in Eq. B.1) describes LexA-regulated synthesis.

As the function $a(\tau,\Psi)$ depends on UV energy fluence, the variable y_0 gives the fluence-time dependence of remained mismatches. In our model these mismatches are considered as a contribution of SOS network to the final mutation frequency. Here to calculate the mutagenesis in individual genes we applied a special model approach.

2.4. A model of UV-induced mutagenesis

The developed model allows quantitative estimation of the mutagenesis in individual genes of *E. coli* bacteria. The yields of UV-induced mutations measured in most cases can be described by the following expression based on the formula introduced by Krasavin and Kozubek (1991):

$$Z_m(\Psi)/Z(\Psi) = \theta_0 + \theta_1\Psi + \theta_2\Psi(1-\exp(-\theta_3\Psi)), \quad (8)$$

where $Z_m(\Psi)$ and $Z(\Psi)$ are the numbers of mutants and survived cells, respectively; Ψ is the energy fluence of UV radiation. The

following interpretation of function components is suggested by Krasavin and Kozubek (1991). The linear component $\theta_1\Psi$ characterizes the mutagenic lesions converted to stable mutations during constitutive repair or DNA replication. This process is seemingly defined by DNA PolIII processing effectiveness (Tang et al., 2000; Borden et al., 2002). $\theta_2\Psi$ is proportional to the yield of premutational (or initial) DNA lesions in an individual gene. $(1-\exp(-\theta_3\Psi))$ is the fraction of mutations induced by mutagenic repair. In our study we have introduced an additional term θ_0 into original formula proposed by Krasavin and Kozubek (1991). This parameter is the constant characterizing spontaneous level of mutagenesis in bacteria defective in some repair functions.

Taking into account the interpretation of terms in Eq. (8) we conclude that a contribution of SOS and MMR systems to the final mutation frequency can be realized only through the θ_3 parameter. Using the models of SOS network, TLS, and MMR, it is possible to determine θ_3 through the variable y_0 (Eq. B.1) which characterizes the amount of mismatches remained after MMR. Therefore, the full chain of events quantitatively described in our model is UV action → thymine dimers → NER and DNA replication → ssDNA → SOS network induction → PolV induction → PolV Mut action with P_{ss} and P_{td} → mismatch induction $a(\tau,\Psi)$ → MMR action → remained mismatches $y_0 \to \theta_3$ parameter → final mutation frequency $Z_m(\Psi)/Z(\Psi)$.

3. Evaluation of the model parameters

The kinetic parameters of the models of the SOS network and TLS were estimated previously (Belov et al., 2009) and presented in Appendix A. Most of the MMR rate constants were determined by fitting the developed model (Eq. B.1) to the *in vitro* experimental data on the MMR kinetics for the 3′ and 5′ pathways (Pluciennik et al., 2009). Other parameters were obtained directly from experimental data or calculated in our previous papers (see Appendix B). To calculate the parameters of UV mutagenesis model we have proposed a special approach described below.

3.1. Parameters of the MMR model

3.1.1. Estimation of parameters for 3′ and 5′ incision

The first group of parameters was evaluated by fitting the model curve for y_8 to experimental data on the MutH-mediated incision stage of MMR (Pluciennik et al., 2009). For the incision in polarity 3′, the parameters k_1, k_2, k_4, k_5, k_6, k_7, and k_8 were estimated. The relation of these dimensional parameters to dimensionless ones (p_i) is presented in the corresponding section of Appendix B. To estimate the first group of parameters, we have set the initial conditions for Eq. (B.1) according to the reactant concentrations for the *in vitro* reaction: $Y_{00}=2.4\times10^{-9}$ M (mismatches), $Y_{01}=3.7\times10^{-8}$ M ($MutS_2$), $Y_{03}=2.5\times10^{-8}$ M ($MutL_2$), and $Y_{05}=1.0\times10^{-9}$ M (MutH). Since the number of GATCm sequences equals the total number of mismatches, we set $Y_{06}=Y_{00}$. Other MMR species were assumed to be zero at $t=0$. The function $a(\tau,\Psi)$ was also set to zero for all t. The dimensionless initial conditions (y_{0i}) for Eq. (B.1) were set respectively. The parameter k_3 was also set to zero for all fitting procedures performed with *in vitro* data. In our model, k_3 is the rate constant of the non-specific losses of $MutS_2$, $MutL_2$, MutH, GATCm, UvrD, exonucleases, PolIII, and DNA ligase in cells growing exponentially. As the contribution of spontaneous protein degradation is negligible for all these species, this parameter has meaning for *in vivo* calculations exclusively. The results of the parameter evaluation for this MMR stage are presented in Fig. 3. The dashed curve corresponds to the y_8 variable recalculated in femtomoles.

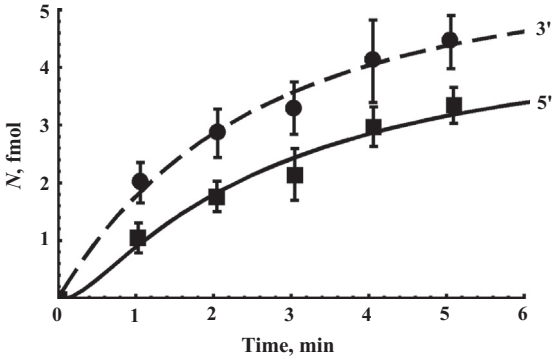

Fig. 3. Incision of a 3′ (•) and 5′ (▪) hemimethylated heteroduplexes by activated MutH in the presence of MutS and MutL. *N* is the concentration of incised DNA. The curves are the calculated results; the dots are the experimental data (Pluciennik et al., 2009).

As it could be concluded from the experimental data (Pluciennik et al., 2009), the rate of MutH-mediated incision is end-specific. To obtain the averaged parameters of this stage for *in vivo* calculations, we have estimated the same set of kinetic rates for the 5′ incision. The initial conditions for Eq. (B.1) were set in the same way as for the 3′ case. The resulting curve compared to experimental data is presented in Fig. 3. The solid line corresponds to y_8 expressed in femtomoles. For the parameters k_1, k_2, k_4, k_5, and k_6, we have obtained the same numerical values as for the 3′ incision. Different values were obtained only for the kinetic rates k_7 and $k_8$characterizing the final MutH-mediated incision event. The ultimate values for the parameters k_7 and $k_8$were calculated by averaging the fitting results for the 3′ and 5′ incisions. The full set of parameters for this MMR stage is presented in Table B.1.

3.1.2. Estimation of the parameters for 3′ and 5′ excision

The second group of parameters was estimated by fitting the model curve y_{14} to experimental data on the excision stage of MMR. To estimate k_{11}, k_{12}, k_{13}, k_{14}, k_{15}, and k_{16}, we have used the data on excision mediated by ExoI (polarity 3′) and RecJ (polarity 5′) (Pluciennik et al., 2009). The initial conditions for Eq. (B.1) were set as follows according to the experimental procedure: $Y_{00}=2.4\times10^{-9}$ M (mismatches), $Y_{01}=3.7\times10^{-8}$ M ($MutS_2$), $Y_{03}=2.5\times10^{-8}$ M ($MutL_2$), $Y_{05}=1.0\times10^{-9}$ M (MutH), $Y_{06}=Y_{00}$ (GATCm), $Y_{09}=1.2\times10^{-8}$ M (UvrD), and $Y_{012}=1.8\times10^{-9}$ M (ExoI). The initial conditions for other species as well as the first term in the equation for y_9 describing the synthesis of UvrD were assumed to be zero. The reaction rates k_1, k_2, k_4, k_5, k_6, k_7, and k_8 were taken from evaluating the 3′ incision stage. The obtained curve corresponding to y_{14} is presented in Fig. 4.

Using experimental data for excision by RecJ, we have obtained the rate constants k_{17}, k_{18}, and k_{19}. The initial conditions for the level of mismatches, $MutS_2$, $MutL_2$, MutH, GATCm, and UvrD were set as for the 3′ excision. For RecJ, we have set $Y_{015}=7.8\times10^{-9}$ M. The resulting curve compared to experimental data is presented in Fug. 4. The values of the estimated parameters for excision stages 3′ and 5′ of MMR are presented in Table B.1.

3.1.3. Estimation of the parameters for the MMR polymerization stage

The last group of parameters was evaluated by fitting the curve for y_{19} to experimental data on single-stranded gap filling by DNA PolIII (Pluciennik et al., 2009). For the case when excision is performed by ExoI, we have set the initial conditions as follows: $Y_{00}=2.4\times10^{-9}$ M (mismatches), $Y_{01}=3.7\times10^{-8}$ M ($MutS_2$), $Y_{03}=2.5\times10^{-8}$ M ($MutL_2$), $Y_{05}=1.0\times10^{-9}$ M (MutH), $Y_{06}=Y_{00}$ (GATCm), $Y_{09}=1.2\times10^{-8}$ M (UvrD), $Y_{012}=1.8\times10^{-9}$ M (ExoI),

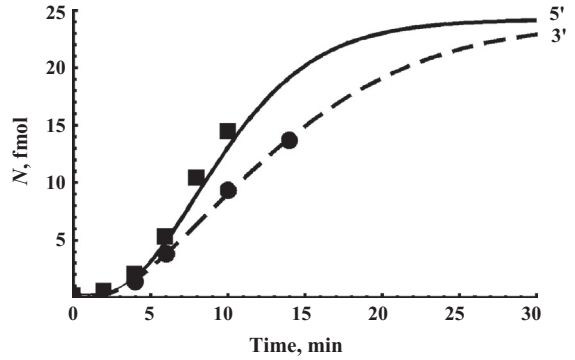

Fig. 4. Excision of a nicked 3′ (•) and 5′ (▪) heteroduplexes by activated ExoI (3′) and RecJ (5′) in the presence of MutS, MutL, DNA helicase II, and SSB. *N* is the concentration of excised DNA. The curves are the calculated results; the dots are the experimental data (Pluciennik et al., 2009).

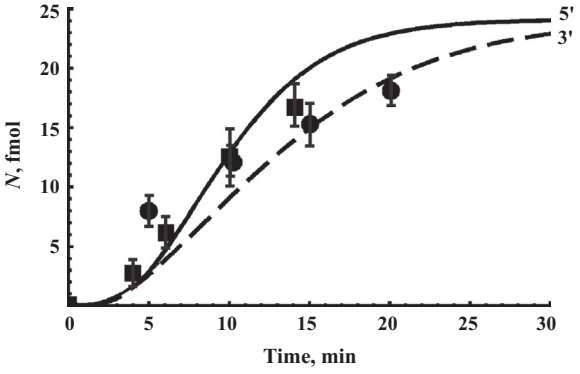

Fig. 5. Gap filling of an excised 3′ (•) and 5′ (▪) heteroduplexes by PolIII. *N* is the concentration of rebuilt DNA. The curves are the calculated results; the dots are the experimental data (Easton and Kushner, 1983).

and $Y_{017}=7.9\times10^{-8}$ M (PolIII). The parameters k_1, k_2, k_4, k_5, k_6, k_7, k_8, k_{11}, k_{12}, k_{13}, k_{14}, k_{15}, and k_{16} were set based on our previous findings. Finally, we have obtained the numerical values for k_{20}, k_{21}, and k_{22}. The dashed curve in Fig. 5 shows the agreement between the calculated curve (y_{19}) and experimental data. The same values of the parameters k_{20}, k_{21}, and k_{22} satisfy the experimental data for single-stranded gap filling, when excision was done by RecJ (see Fig. 5). In this case, we have set the same initial conditions except the levels of ExoI and RecJ: $Y_{012}=0$ (ExoI), $Y_{015}=7.8\times10^{-9}$ M (RecJ). The set of the newly obtained parameters is presented in Table B.1.

3.2. Estimation of the UV mutagenesis model parameters

3.2.1. θ_0, θ_1, and θ_2 parameters

The parameter θ_0 depends on the bacteria strain and can be estimated directly from experimental data. For the strains with normal DNA repair functions, we assume this parameter to be zero. For the strains containing a mutation in either *mutS*, *mutL*, or *mutH* gene, we have set the corresponding values of $\theta_{0,\ mutS}$, $\theta_{0,\ mutL}$, and $\theta_{0,\ mutH}$ according to the experimental data (Hongbo et al., 2000). For the strain defective both in *umu* and *mut* genes, we have set the corresponding value for $\theta_{0,\ umu,\ mut}$ from the same paper. The coefficient θ_1 of the linear component in Eq. (8) can be defined as the mutagenic effectiveness of DNA PolIII processing according to Drake (1969) (see Appendix C).

The coefficient θ_2 characterizing the number of premutational lesions in a gene is defined as follows in our model. Let us assume that L_1 base pairs is the length of a gene, L_0 is the length of *E. coli's* whole genome, and m_0 is the yield of the initial lesions per full bacterial chromosome. Then the average number of premutational DNA lesions in a gene is $\theta_2=L_1m_0/L_0$. As we are estimating the mutation frequency in the *lacZ* gene, we have to assign the corresponding length of this gene and the length of *E. coli's* whole K-12 MG1655 genome (Table C.1).

3.2.2. θ_3 parameter for mut$^+$ bacterial strains

To estimate the parameter θ_3 through which the SOS and MMR systems contribute to the final mutation frequency, we used the following assumptions. The dependence of y_0 on UV energy fluence can be approximated by a linear function with a certain slope coefficient k_s. Such approximation is suitable for any time point within the calculation interval. The obtained slope coefficient is proportional to the parameter θ_3. However, the meaning of θ_3 implies finding the exact form of this proportionality. As we are calculating the yield of the mutations produced exclusively in an individual *E. coli's* gene, we should take into account only the mismatches remaining within the length of this gene. Therefore, the final expression for this parameter will be $\theta_3=L_1k_s/L_0$.

To find the numerical value for θ_3, we performed the following procedure consisting in running simultaneously models of the SOS-network, TLS, and MMR with corresponding sets of parameters and initial conditions. First, using the SOS network model, we have calculated the fluence-time dependence for PolV represented as the variable x_{11} (Fig. 6). The SOS network model was computed using Eqs. (1) and (A.1). The initial conditions and kinetic parameters were set as described in Appendix A. Then,

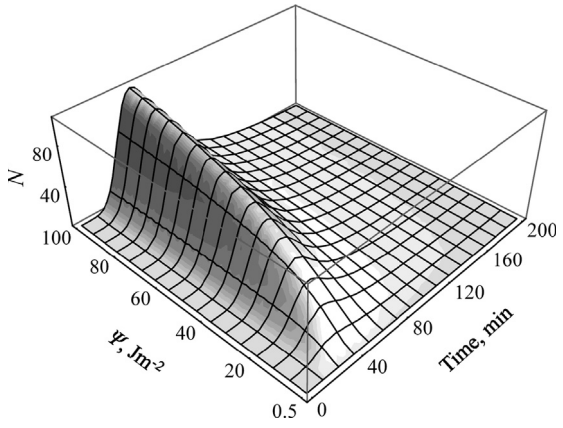

Fig. 6. Three-dimensional plot showing the PolV level change with time and depending on the UV energy fluence. *N* is the number of PolV molecules per one cell.

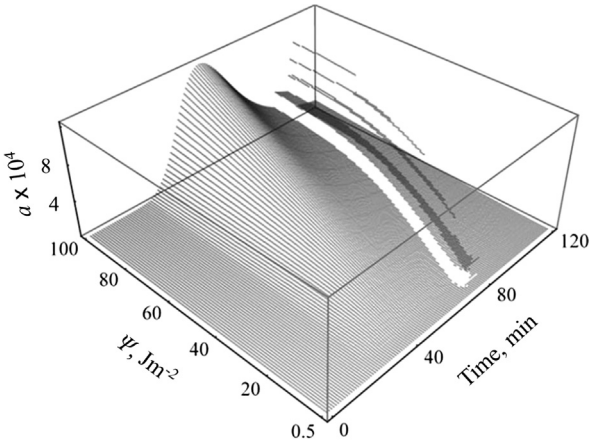

Fig. 7. Dependence of the mean number of the occurring mismatches *a* on time and UV energy fluence.

using the TLS model, we have estimated the function $a(\tau,\Psi)$ (Fig. 7). Here we used Eqs. (3)–(7) of this model implemented in the developed program code. The parameters for this calculation are also presented in Appendix A. This code gives discrete values for $a(\tau,\Psi)$ to reflect the specifics of nucleotide pasting by PolV Mut. The first large peak of the function $a(\tau,\Psi)$ is caused by processing the over-produced PolV Mut molecules at undamaged DNA sites; other disturbances are caused by the process of thymine dimer bypass (Belov et al., 2009). The energy fluence range for these calculations was set as in Belov et al. (2009): $0.5 \le \Psi \le 100\ Jm^{-2}$. To compute all ODE systems presented in this paper, we have used the fourth-order Runge–Kutta method.

After that, we have calculated the dependence of the remaining mismatches y_0 on UV energy fluence and on time using the MMR model (Fig. 8). Since we use the function $a(\tau,\Psi)$ as the input data, we obtain the discrete values for y_0 as well. The MMR model was initialized with the kinetic parameters estimated earlier from the fitting procedure (Table B.1). The *in vivo* data on the normal intracellular levels of all MMR proteins were used as the initial conditions for calculating $y_0(\tau,\Psi)$. The numerical values for Y_{01} ($MutS_2$), Y_{03} ($MutL_2$), Y_{05} (MutH), Y_{09} (UvrD), Y_{012} (3′ exonucleases), Y_{015} (5′ exonucleases), Y_{017} (PolIII), and Y_{021} (DNA ligase) are estimated directly from experimental data and summarized in Table B.1. As we assume an equal probability of each pathway corresponding to different exonuclease activity, we set the normal intracellular levels of 3′ and 5′ exonucleases as follows: $Y_{012} = [\text{ExoI}] + 0.5[\text{ExoVII}] + [\text{ExoX}]$, $Y_{015} = 0.5[\text{ExoVII}] + [\text{RecJ}]$. The initial level of mismatches was set as $Y_{00} = a(0,\Psi) = 0$.

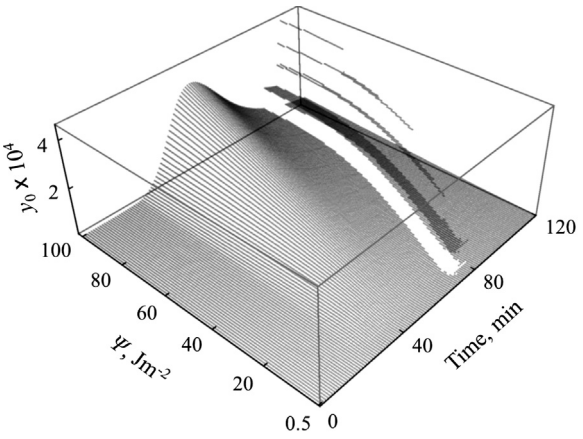

Fig. 8. Dependence of the remained mismatches y_0 on time and UV energy fluence for strains with normal MMR functioning.

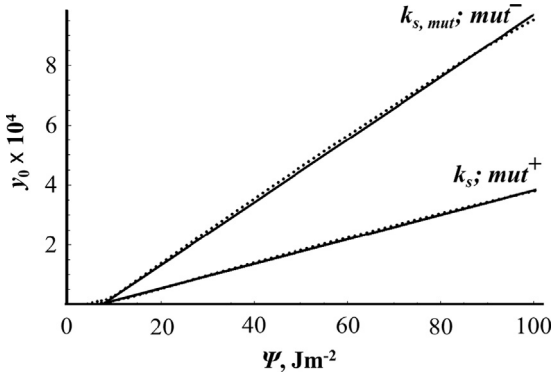

Fig. 9. Approximation of the obtained $y_0(\tau,\Psi)$ dependence by linear functions with the slope coefficients for the strains with normal repair functions ($k_s = 4.1 \times 10^{-6}$) and for the mut^- strains ($k_{s,\ mut} = 1.05 \times 10^{-5}$). The dotted lines represent $y_0(\tau,\Psi)$ values at the moment corresponding to maximal concentration of PolV. The solid lines represent linear approximation.

At the next step, we have approximated the obtained $y_0(\tau,\Psi)$ dependence by a linear function with the slope coefficient k_s. The approximation was carried out at the time point corresponding to the maximal concentrations of PolV (Fig. 9). Using the parameter k_s, we have obtained the numerical value of θ_3 (see Table C.1).

3.2.3. Parameters $\theta_{3,\ mut}$, $\theta_{3,\ umu}$ for mut^- and umu^- bacterial strains

To calculate the parameter $\theta_{3,\ mut}$ for bacteria defective in the MMR function, we have used the same procedure as for θ_3 except for the different set of initial conditions for the MMR model. For the strains defective in either *mutS*, *mutL*, or *mutH* gene, we have set to zero the initial levels of the corresponding proteins: $mutS^-$, $Y_{01} = 0$; $mutL^-$, $Y_{03} = 0$; $mutH^-$, $Y_{05} = 0$. For all the mutants, we obtained the identical value of the slope coefficient $k_{s,\ mut}$ and then $\theta_{3,\ mut}$ (Table C.1).

We also estimated the parameter $\theta_{3,\ umu}$ for the umu^- strains containing a mutation in the *umu*-genes of *E. coli*. This mutation prevents the formation of PolV complex and, therefore, leads to the absence of the mutagenic effect of SOS repair. Here we set to zero the initial levels of either UmuD or UmuC protein in the SOS network model: $X_{04} = 0$ or $X_{05} = 0$, respectively. In both cases, we have obtained $\theta_{3,\ umu} = 0$. For the umu^- mut^- bacterial strains defective in both SOS and MMR systems, we also obtained $\theta_{3,\ umu,\ mut} = 0$.

4. Calculation of UV-induced mutagenesis

Using our model we have performed calculations of the mutation frequency in *E. coli* strains with different genotypes. The mutagenic effect of UV radiation was modeled for the cells with normal SOS and MMR functions and for mutants defective in different MMR genes. In this study, we have estimated the mutation frequency in the *E. coli's lacZ* gene encoding β-galactosidase. The results of modeling were compared with experimental data on the revertant frequency in two alleles at *lacZ* codon 461, which reverts via **CCC**→**CTC** and CT**T**→CT**C** transitions (Hongbo et al., 2000).

4.1. Mutagenesis in bacteria with the normal SOS and MMR functions

First, we have simulated the UV-induced mutation frequency for the strains with the normal functioning of the SOS and MMR systems. The final mutation frequency was calculated by Eq. (8) using the parameter θ_3. As we obtained a linear dependence of θ_3 on UV energy fluence (Fig. 9), we can extend the range of Ψ for calculations with formula (8) and start calculations of the mutation frequency at $\Psi = 0\ Jm^{-2}$. The parameter θ_0 can be neglected in this case. Therefore, we set it to zero. The coefficients θ_1 and θ_2 are the same for the normal and mutagenic strains (Table C.1). The results of calculation for bacteria with the normal functioning of the SOS system and MMR are presented in Fig. 10 and indicated as mut^+. The corresponding experimental data are also shown in this plot (Hongbo et al., 2000).

4.2. Mutagenesis in bacteria defective in MMR functions

4.2.1. Calculations for $mutS^-$ strains

To estimate the UV-induced mutation frequency for the $mutS^-$ mutant strains, we have used the same θ_1 and θ_2 parameter values as for cells with normal MMR. The parameter $\theta_{0,\ mutS}$ was set according to the spontaneous mutation rate demonstrated by the $mutS^-$ strains (Hongbo et al., 2000). Therefore, at $\Psi = 0\ J/m^2$, the curve computed

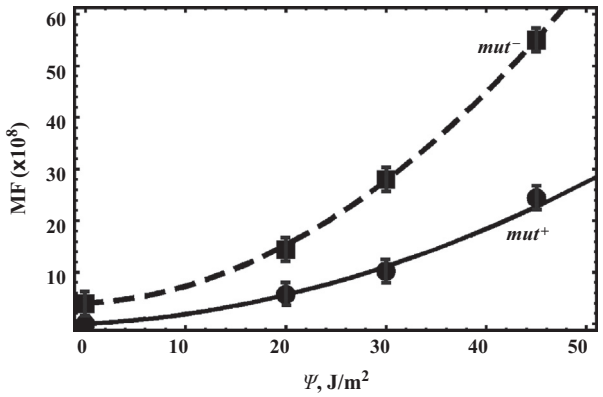

Fig. 10. Dependence of the mutation frequency on UV energy fluence calculated for mut^+ (the solid line) and $mutS^-$ (the dashed line) strains. The symbols represent experimental data for mut^+ (•) and $mutS^-$ (▪) strains (Hongbo et al., 2000). The experimental data with their standard errors of the means ($\times 10^{-8}$) for mut^+ and $mutS^-$, are, respectively, 0 J/m^2, 0, 4.0 ± 0.4; 20 J/m^2, 14.4 ± 0.9, 5.7 ± 0.2; 30 J/m^2, 28.0 ± 3.4, 10.2 ± 0.9; 45 J/m^2, 55.0 ± 1.0, 24.4 ± 4.2.

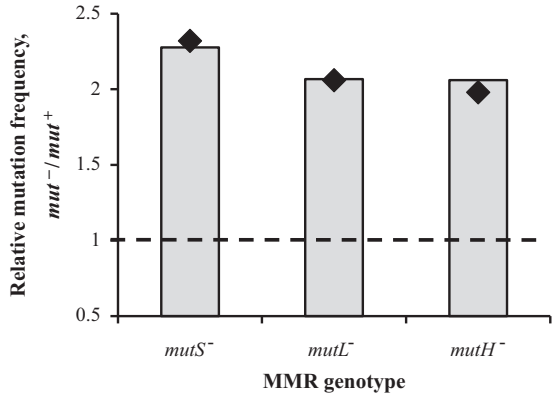

Fig. 11. Mutation frequency in bacteria defective in the *mutL* and *mutH* functions at the UV energy fluence of 30 J/m^2. The bars are experimental data (Hongbo et al., 2000); the symbols are the calculated mutation frequency.

for these strains starts from a nonzero level. The parameter $\theta_{3,\ mut}$ was chosen as described in Section 3.2. In our calculations, we have obtained on the average the 2.6-fold increase in the mutation frequency in a $mutS^-$ strain as compared with a mut^+ one (Fig. 10). In other words, we have shown that MMR reduces the mutation rate by 2.6 times. The results of calculations are in accordance with the experimental data (Hongbo et al., 2000).

4.2.2. *Mutagenesis in mut⁻ strains for a single value of UV energy fluence*

In this section, we present the results of calculations for $mutL^-$ and $mutH^-$ bacteria at a single UV energy fluence of 30 J/m^2 (Fig. 11). The results obtained for these strains are about two times higher than for mut^+ ones — just like in the experiment (Hongbo et al., 2000). Taking into account the experimental standard errors of means (SEM), we can conclude that the model adequately reconstructs the observed mutagenic effect. Here we used the same θ_1, θ_2, and $\theta_{3,\ mut}$ parameter values as for $mutS^-$ strains. The difference is only in choosing the parameter θ_0, which characterizes the spontaneous level of mutagenesis demonstrated by a strain. For $mutL^-$ and $mutH^-$ bacteria, we used $\theta_{0,\ mutL}$ and $\theta_{0,\ mutH}$ chosen according to the experimental data (Hongbo et al., 2000). Despite the equivalent contribution of the SOS and MMR models to formula (8), we have different levels of the mutation frequency for the $mutS^-$, $mutL^-$, and $mutH^-$ mutants due to different spontaneous mutagenesis defined by the parameters $\theta_{0,\ mutS}$, $\theta_{0,\ mutL}$, and $\theta_{0,\ mutH}$, respectively.

4.3. *Mutagenesis in bacteria defective both in SOS and MMR functions*

As it is known, a defect in some of *umuDC* genes leads to the inactivation of the SOS function because it prevents the normal assembling of UmuD'$_2$C complex, which is the main component of PolV Mut. In our model, we reconstructed the mutagenic effect observed experimentally with the simultaneous defects in the *umuC* and *mut* genes.

Setting the parameter $\theta_{0,\ umu,\ mut}$ according to the average spontaneous mutation frequency for the umu^-mut^- strains, we have calculated the level of mutagenesis to be ~5.7×10^{-8}, which is close to experimental data (Hongbo et al., 2000). In this case, the SOS and MMR systems do not contribute to formula (8) because $\theta_{3,\ umu,\ mut}=0$. Therefore, the level of mutagenesis is determined only by the parameters $\theta_{0,\ umu,\ mut}$ and θ_1.

5. Discussion

The model approach described here has attempted to show one possible mechanistic explanation of the experimentally observed reduction in UV-induced mutation rate which can be connected with the action of MMR system. Our model meets the hypothesis on the possible role of the MMR in radiation-induced SOS mutagenesis. Choosing UV radiation as a mutagenic factor for this study is explained by the necessity to indicate the links between MMR and SOS response without any significant influence of other repair systems such as single- and double-strand break repair and base excision repair. Since most of the UV-induced thymine dimers not removed by NER represent a substrate for SOS repair, it gives an opportunity to identify the direct connections between the biochemical mechanisms of these two systems.

The developed models provide a topological view of the MMR and SOS networks attempted to clarify their biological relations. Using our mathematical approach, we have analyzed all the chain of events from the primary DNA lesion appearance to fixing this lesion as a mutation. The model adequately describes the basic processes of the SOS response and MMR. Mathematical description of these two systems is carried out in compliance with concepts of modern system biology and with simulation methods of studying complex genetic networks.

A special issue should be addressed: the possible feedback of MMR to the SOS network. There are two major stages which could be considered as its possible pathways. The first one is the involvement of UvrD in MMR. As it is known, the synthesis of this protein is regulated by the LexA repressor and, therefore, the level of UvrD increases after UV irradiation. However, the amount of UvrD helicase molecules necessary for successful MMR functioning is not large (one molecule per one mismatch). Therefore, the interactions of UvrD during MMR should not affect the SOS network significantly. Strictly speaking, UvrD is not involved directly in the SOS system. It is one of the major NER proteins which precedes SOS induction. Another possible feedback mechanism is the production of single-stranded DNA regions created during MMR. There is no experimentally confirmed clear evidence of the impact of these ssDNA sites on the SOS network functioning. Taking into account the specific conformation of the protein–DNA complexes formed during MMR, we can suppose that it has a protective effect that prevents the RecA protein binding to single-stranded sites. Therefore, on the basis of these conclusions, we do not suggest that there is any feedback for MMR within our model.

In this paper, we have shown how more or fewer functions connected with the activity of the *mut* and *umu* genes affect the mutation frequency, *i.e.* what influence the system's different topologies have on the final cell response to irradiation. Here we have provided a possible mechanistic explanation of how a violation of the expression of these genes leads to an increase in mutagenesis in bacterial cells. It is clear that this method can be extrapolated to other SOS genes responsible for assembling the PolV Mut complex. According to our model, violations in the *umuD* or *recA* gene result in the same mutation frequency as in *umuC*-defective strains.

Besides our previous studies, only a few papers are concerned with simulating some quantitative characteristics of TLS (Vaidyanathan and Cho, 2012; Malina et al., 2012). However, these approaches do not provide a system view of the process as well as do not focus on its probabilistic aspects and connections with other repair systems. One of the main features of our models is a clear representation of cause-and-effect relations between two complicate repair networks and the TLS effectiveness. In addition to the quantitative analysis of mutagenic effects, the developed models provide a tool for the detailed analysis of the protein–protein interaction dynamics of the SOS network and MMR system.

In this paper, we focused mainly on the problem of induced mutagenesis. Here we did not include a special mathematical description of the effects that contribute to spontaneous mutagenesis. This is the main reason for using the classical formula for the estimation of the final mutation frequency. The comprehensive reconstruction of the whole mutation process based only on mechanistic models requires the development of additional model approaches for other repair systems. Therefore, we used a more suitable approach based on modeling the biophysical processes behind the parameters of the classical equation.

Taking into account the knowledge of the molecular mechanisms of other *E. coli's* repair systems, we suggest that our model could be applied for the estimation of mutagenesis induced not only by UV radiation but also by ionizing radiations of different quality. The latter relates mostly to the repair of charged particle-induced clustered DNA lesions because it is supposed that these lesions make up the main substrate for mutagenic SOS repair.

Acknowledgments

This study was performed within the research project # 301 “Mathematical Modelling of Genetic Regulatory Networks in Bacterial and Higher Eukaryotic Cells” between Laboratory of Radiation Biology of Joint Institute for Nuclear Research and Cairo University. O. Chuluunbaatar acknowledges a financial support from the RFBR Grant no. 11-01-00523, and the JINR theme 09-6-1060–2005/2013 “Mathematical Support of experimental and theoretical studies conducted by JINR”.

Appendix A. Details of SOS network and TLS models

Equations of the SOS network model

The equations reflecting the dynamical change of SOS protein's concentration are designed in our previous study (Belov et al., 2009):

$$\frac{dx_1}{d\tau} = \frac{x_{01}(1+q_5^{h_1})}{1+(x_1/\gamma_1 N_A)^{h_1}} - q_6 x_1 x_3 - x_1,$$

$$\frac{dx_2}{d\tau} = \frac{x_{02}(1+q_7^{h_2})}{1+(x_1/\gamma_2 N_A)^{h_2}} + q_1 x_3 - q_8 x_0 x_2 - x_2,$$

Table A.1
Parameters of SOS network and TLS models.

Parameter	Value	Reference
α	0.0116 min^{-1}	Aksenov et al. (1997)
t_1	0.17 min	Aksenov et al. (1997)
T_0	40 min	Aksenov et al. (1997)
υ_1	0.7 min^{-1}	Aksenov et al. (1997)
l_1	900 nucleotides	Aksenov et al. (1997)
ε	7.7×10^4 M	Belov et al. (2009)
δ_4	0.0231 min^{-1}	Belov et al. (2009)
δ_5	0.0347 min^{-1}	Belov et al. (2009)
δ_6	0.0173 min^{-1}	Belov et al. (2009)
δ_7	0.0154 min^{-1}	Belov et al. (2009)
δ_8	0.0116 min^{-1}	Belov et al. (2009)
δ_9	0.0107 min^{-1}	Belov et al. (2009)
δ_{10}	0.0224 min^{-1}	Belov et al. (2009)
δ_{11}	0.0116 min^{-1}	Belov et al. (2009)
δ_{12}	0.0154 min^{-1}	Belov et al. (2009)
σ_1	1.1×10^5 $M^{-1}min^{-1}$	Belov et al. (2009)
σ_2	7.7×10^4 $M^{-1}min^{-1}$	Belov et al. (2009)
β_2	3.7×10^5 $M^{-1}min^{-1}$	Aksenov et al. (1997)
β_3	1.9×10^3 $M^{-1}min^{-1}$	Belov et al. (2009)
η	4.0×10^4 $M^{-1}min^{-1}$	Belov et al. (2009)
μ	5.8×10^4 $M^{-1}min^{-1}$	Belov et al. (2009)
φ	3.9×10^4 $M^{-1}min^{-1}$	Belov et al. (2009)
a_1	6.2×105 $M^{-1}min^{-1}$	Belov et al. (2009)
a_2	4.6×10^5 $M^{-1}min^{-1}$	Belov et al. (2009)
a_3	4.3×10^5 $M^{-1}min^{-1}$	Belov et al. (2009)
b_2	3.9×10^4 $M^{-1}min^{-1}$	Belov et al. (2009)
γ_1	2.0×10^{-8} M	Aksenov et al. (1997)
γ_2	2.0×10^{-9} M	Aksenov et al. (1997)
γ_4	5.5×10^{-7} M	Aksenov et al. (1997)
γ_5	2.0×10^{-10} M	Aksenov et al. (1997)
h_1	2.6	Belov et al. (2009)
h_2	2	Aksenov et al. (1997)
h_4	2	Belov et al. (2009)
h_5	2	Belov et al. (2009)
X_{01}	2.2×10^{-6} M	Hegde et al. (1995)
X_{02}	1.19×10^{-5} M	Bianco and Kowalczykowski (1999)
X_{04}	2.99×10^{-7} M	Sassanfar and Roberts (1990)
X_{05}	2.49×10^{-8} M	Goodman and Woodgate (2000)
X_{07}	2.24×10^{-7} M	Belov et al. (2009)
X_{010}	1.54×10^{-7} M	Belov et al. (2009)
v_{ss}	16.8 nucleotides per min	Fujii and Fuchs (2004)

$$\frac{dx_3}{d\tau} = q_8 x_0 x_2 - q_1 x_3,$$

$$\frac{dx_4}{d\tau} = \frac{x_{04} q_9 (1+q_{10}{}^{h_4})}{1+(x_1/\gamma_4 N_A)^{h_4}} + q_{11} x_6 x_{10} + q_{12} x_6 x_7 + q_{13} x_6 - q_{14} x_4 x_3 - q_{15} x_4^2 - q_{16} x_4 x_8 - q_{17} x_4 x_6 - q_{18} x_4 x_{11} - q_{19} x_4,$$

$$\frac{dx_5}{d\tau} = \frac{x_{05} q_{20} (1+q_{21}{}^{h_5})}{1+(x_1/\gamma_5 N_A)^{h_5}} - q_{22} x_5 x_7 - q_{23} x_5 x_8 - q_{24} x_5 x_9 - q_{25} x_5,$$

$$\frac{dx_6}{d\tau} = q_{14} x_3 x_4 + q_{16} x_4 x_8 + q_{18} x_4 x_{11} - q_{26} x_6^2 - q_{17} x_4 x_6 - q_{11} x_6 x_{10} - q_{12} x_6 x_7 - q_{13} x_6,$$

$$\frac{dx_7}{d\tau} = q_{15} x_4^2 - q_{22} x_5 x_7 - q_{12} x_6 x_7 - q_{27} x_7,$$

$$\frac{dx_8}{d\tau} = q_{26} x_6^2 - q_{16} x_4 x_8 - q_{23} x_5 x_8 - q_{28} x_8,$$

$$\frac{dx_9}{d\tau} = q_{17} x_4 x_6 + q_{16} x_4 x_8 + q_{12} x_6 x_7 - q_{24} x_5 x_9 - q_{29} x_9,$$

$$\frac{dx_{10}}{d\tau} = q_{22} x_5 x_7 - q_{11} x_6 x_{10} - q_{30} x_{10},$$

$$\frac{dx_{11}}{d\tau} = q_{23} x_5 x_8 - q_{18} x_4 x_{11} - q_{31} x_{11},$$

$$\frac{dx_{12}}{d\tau} = q_{24} x_5 x_9 + q_{18} x_4 x_{11} + q_{11} x_6 x_{10} - q_{32} x_{12}. \quad (A.1)$$

The initial conditions for this model are the following:

$x_1(0)=x_{01}$, $x_2(0)=x_{02}$, $x_3(0)=0$, $x_4(0)=x_{04}$, $x_5(0)=x_{05}$, $x_6(0)=0$, $x_7(0)=x_{07}$, $x_8(0)=0$, $x_9(0)=0$, $x_{10}(0)=x_{010}$, $x_{11}(0)=0$, $x_{12}(0)=0$.

In Eq. (A.1), $x_1, x_2, x_3, x_4, x_5, x_6, x_7, x_8, x_9, x_{10}, x_{11}$, and x_{12} are the normalized intracellular concentrations of the LexA, RecA, RecA*, UmuD, UmuC, UmuD′, $UmuD_2$, $UmuD'_2$, UmuDD′, $UmuD_2C$, $UmuD'_2C$, and UmuDD′*C* proteins, respectively; q_j $(j=1,\ldots,m)$ is the normalized constant of the *j*-th protein–protein interaction.

Kinetic parameters of the SOS network model

(1) The parameters of Eq. (1): $\tau=\alpha t$, $\tau_2=\alpha t_2$, $q_1=\delta_3(\Psi)/\alpha$, $q_2=25t_1/T_0$, $q_3=\upsilon_1/\alpha$, $q_4=\upsilon_1 T_0$. T_0 is replication duration at the normal growth conditions, α is the rate constant of the processes of the nonspecific loss of the *lexA* gene product; N_A is the Avogadro constant; l_1 is an average length of a single-stranded DNA gap formed during the replication of sites containing thymine photodimers, and t_2 is the replication termination time. For $\delta_3(\Psi)$ the following expression takes place (Belov et al., 2009):

$$\delta_3(\Psi)=0.147\ \exp\left(\frac{1}{1+0.359\Psi}\right)\ \mathrm{min}^{-1}.$$

(2) The parameters of Eq. (A.1): $x_i=X_iN_A$ $(i=1,\ldots,12)$, $q_5=X_{01}/\gamma_1$, $q_6=\delta_3(\Psi)/(X_{01}\alpha N_A)$, $q_7=X_{01}/\gamma_2$, $q_8=\beta_2 50 l_1/(T_0\alpha^2 N_A)$, $q_9=(\varepsilon X_{04}+\delta_4)/\alpha$, $q_{10}=X_{01}/\gamma_4$, $q_{11}=\sigma_1/(\alpha N_A)$, $q_{12}=\sigma_2/(\alpha N_A)$, $q_{13}=\delta_6/\alpha$, $q_{14}=\beta_3/(\alpha N_A)$, $q_{15}=\varepsilon/(\alpha N_A)$, $q_{16}=\varphi/(\alpha N_A)$, $q_{17}=\mu/(\alpha N_A)$, $q_{18}=b_2/(\alpha N_A)$, $q_{19}=\delta_4/\alpha$, $q_{20}=(a_1X_{07}+\delta_5)/\alpha$, $q_{21}=X_{01}/\gamma_5$, $q_{22}=a_1/(\alpha N_A)$, $q_{23}=a_2/(\alpha N_A)$, $q_{24}=a_3/(\alpha N_A)$, $q_{25}=\delta_5/\alpha$, $q_{26}=\eta/(\alpha N_A)$, $q_{27}=\delta_7/\alpha$, $q_{28}=\delta_8/\alpha$, $q_{29}=\delta_9/\alpha$, $q_{30}=\delta_{10}/\alpha$, $q_{31}=\delta_{11}/\alpha$, $q_{32}=\delta_{12}/\alpha$. Here $x_{01}=X_{01}/X_{01}=1$, $x_{02}=X_{02}/X_{01}$, $x_{04}=X_{04}/X_{01}$, $x_{05}=X_{05}/X_{01}$, $x_{07}=X_{07}/X_{01}$, and $x_{010}=X_{010}/X_{01}$ are constitutive concentrations of the LexA, RecA, UmuD, UmuC, $UmuD_2$ and $UmuD_2C$ proteins, respectively (Table A.1).

Parameters of the TLS model

The translesion synthesis model has the following parameter values: $P_{ss}=2.1\times10^{-4}$ (Belov et al., 2009), $P_A=0.875$, $P_B=0.078$, $P_C=0.02$, and $P_D=0.048$ (Tang et al., 2000; Livneh, 2000). We conclude that if we consider any of the two basic UV-induced DNA lesions (either TT (6–4) photoproduct—20% or *cys–syn* cyclobutane photodimer—80% (Wang, 1976; Cadet and Vigny, 1990)), then the 3′-end or 5′-end lesions are equally probable. Therefore, according to Eq. (7), the probabilities of generating each of the four types of lesions were found to be $P_1=P_2=0.1$, $P_3=P_4=0.4$, and $P_{td}=0.12$.

Appendix B. MMR model details

Equations of the MMR model

The dynamical change of MMR protein's concentrations is described by the following system of ordinary differential equations:

$$\begin{aligned}
\frac{dy_0}{d\tau}&=a(\tau,\Psi)-p_1y_0y_1+p_2y_2,\\
\frac{dy_1}{d\tau}&=y_{01}-y_1(p_3+p_1y_0)+p_{13}y_{10}+p_2y_2,\\
\frac{dy_2}{d\tau}&=p_1y_0y_1-y_2(p_2+p_4y_3)+p_5y_4,\\
\frac{dy_3}{d\tau}&=y_{03}+p_{13}y_{10}-y_3(p_3+p_4y_2)+p_5y_4,\\
\frac{dy_4}{d\tau}&=p_4y_2y_3-y_4(p_5+p_8y_7),\\
\frac{dy_5}{d\tau}&=y_{05}+p_{13}y_{10}-y_5(p_3+p_6y_6)+p_7y_7,\\
\frac{dy_6}{d\tau}&=y_{06}+p_{13}y_{10}-y_6(p_3+p_6y_5)+p_7y_7,\\
\frac{dy_7}{d\tau}&=p_6y_5y_6-y_7(p_7+p_8y_4),\\
\frac{dy_8}{d\tau}&=p_{12}y_{10}+p_8y_4y_7-p_{11}y_8y_9,\\
\frac{dy_9}{d\tau}&=\frac{p_3y_{09}(1+p_9^{h_9})}{1+(p_{10}x_1)^{h_9}}+y_{10}(p_{12}+p_{13})-y_9(p_3+p_{11}y_8),\\
\frac{dy_{10}}{d\tau}&=p_{11}y_8y_9-y_{10}(p_{12}+p_{13}),\\
\frac{dy_{11}}{d\tau}&=p_{13}y_{10}-y_{11}(p_{14}y_{12}+p_{17}y_{15})+p_{15}y_{13}+p_{18}y_{16},\\
\frac{dy_{12}}{d\tau}&=y_{012}-y_{12}(p_3+p_{14}y_{11})+y_{13}(p_{15}+p_{16}),\\
\frac{dy_{13}}{d\tau}&=p_{14}y_{11}y_{12}-y_{13}(p_{15}+p_{16}),\\
\frac{dy_{14}}{d\tau}&=p_{16}y_{13}-p_{19}y_{16}-p_{20}y_{14}y_{17}+p_{21}y_{18},\\
\frac{dy_{15}}{d\tau}&=y_{015}-y_{15}(p_3+p_{17}y_{11})+y_{16}(p_{18}+p_{19}),\\
\frac{dy_{16}}{d\tau}&=p_{17}y_{11}y_{15}-y_{16}(p_{18}+p_{19}),\\
\frac{dy_{17}}{d\tau}&=y_{017}-y_{17}(p_3+p_{20}y_{14})+y_{18}(p_{21}+p_{22}),\\
\frac{dy_{18}}{d\tau}&=p_{20}y_{14}y_{17}-y_{18}(p_{21}+p_{22}),\\
\frac{dy_{19}}{d\tau}&=p_{22}y_{18}-p_{23}y_{19}y_{20}+p_{24}y_{21},\\
\frac{dy_{20}}{d\tau}&=y_{020}-y_{20}(p_3+p_{23}y_{19})+y_{21}(p_{24}+p_{25}),\\
\frac{dy_{21}}{d\tau}&=p_{23}y_{19}y_{20}-y_{21}(p_{24}+p_{25}),\\
\frac{dy_{22}}{d\tau}&=p_{25}y_{21}.
\end{aligned}\tag{B.1}$$

The initial conditions for this system are the following:

$y_0(0)=0$, $y_1(0)=y_{01}$, $y_2(0)=0$, $y_3(0)=y_{03}$, $y_4(0)=0$, $y_5(0)=y_{05}$, $y_6(0)=y_{06}$, $y_7(0)=0$, $y_8(0)=0$, $y_9(0)=y_{09}$, $y_{10}(0)=0$, $y_{11}(0)=0$, $y_{12}(0)=y_{012}$, $y_{13}(0)=0$, $y_{14}(0)=0$, $y_{15}(0)=y_{015}$, $y_{16}(0)=0$, $y_{17}(0)=y_{017}$, $y_{18}(0)=0$, $y_{19}(0)=0$, $y_{20}(0)=y_{020}$, $y_{21}(0)=0$, $y_{22}(0)=0$.

In Eq. (B.1) y_0 is the normalized intracellular level of the mismatches (Mism). $a(\tau,\Psi)$ is the function describing the increase of mismatches produced by the PolV Mut complex. y_1 is the concentration of the MutS dimer, which recognizes a mismatch and binds to it reversibly forming an intermediate $MismMutS_2$ complex (y_2). y_3 represents the normalized concentration of the MutL dimer, which joins the $MismMutS_2$ complex and forms the next intermediate $MismMutS_2L_2$ (y_4). y_5 is the concentration of the MutH protein interacting with the methylated GATCm sequence (y_6) with the production of the GATCmMutH complex (y_7). y_8 represents the level of nicked DNA after the interaction of $MismMutS_2L_2$ complexes with GATCmMutH. The molecules of the $MutS_2$, $MutL_2$, and MutH proteins remain joined to the nicked DNA strand. The following strand unwinding by the UvrD-helicase (y_9) can be represented as a typical enzymatic reaction with the intermediate complex y_{10} and resulting detachment of $MutS_2$, $MutL_2$, MutH, and UvrD. Since the synthesis of the UvrD helicase is SOS-dependent, we introduced the normalized concentration of the LexA protein (x_1) into the equation for y_9. The kinetics of LexA is calculated using the model of SOS network (Eq. A.1). The action of UvrD leads to the formation of an unwound DNA sequence y_{11} which will be processed by two pathways with different exonucleases demonstrating 3′ or 5′ polarity. Here we assign the variables y_{12} and y_{15} to the levels of 3′ (ExoI, ExoVII, ExoX) and

Table B.1
Parameters of MMR model.

Parameter	Value	Reference
k_1	5.2×10^7 M^{-1} min^{-1}	This paper
k_2	0.195 min^{-1}	This paper
k_3	0.0116 min^{-1}	Aksenov et al. (1997)
k_4	1.3×10^3 M^{-1} min^{-1}	This paper
k_5	0.118 min^{-1}	This paper
k_6	1.4×10^8 M^{-1} min^{-1}	This paper
k_7	0.088 min^{-1}	This paper
k_8	7.0×10^7 M^{-1} min^{-1}	This paper
k_{11}	3.3×10^{-4} min^{-1}	This paper
k_{12}	0.045 min^{-1}	This paper
k_{13}	0.22 l min^{-1}	This paper
k_{14}	3.3×10^{-4} min^{-1}	This paper
k_{15}	1.4×10^{-4} min^{-1}	This paper
k_{16}	0.124 min^{-1}	This paper
k_{17}	6.7×10^4 M^{-1} min^{-1}	This paper
k_{18}	0.151 min^{-1}	This paper
k_{19}	0.255 min^{-1}	This paper
k_{20}	3.9×10^7 M^{-1} min^{-1}	This paper
k_{21}	0.052 min^{-1}	This paper
k_{22}	0.092 min^{-1}	This paper
k_{23}	1.8×10^6 M^{-1} min^{-1}	Belov (2011)
k_{24}	0.067 min^{-1}	Belov (2011)
k_{25}	0.02 l min^{-1}	Belov (2011)
γ_9	1.4×10^{-7} M	Belov et al. (2009), Viswanathan and Lovett (1999)
h_9	2	Aksenov et al. (1997)
Y_{01}	3.1×10^{-7} M	Feng et al. (1996)
Y_{02}	1.9×10^{-7} M	Feng et al. (1996)
Y_{05}	2.2×10^{-7} M	Feng et al. (1996)
Y_{09}	5.0×10^{-6} M	Petit et al. (1998)
Y_{012}	8.9×10^{-5} M	Cooper et al. (1993), Viswanathan and Lovett (1999)
Y_{015}	6.3×10^{-8} M	Cooper et al. (1993), Haggerty and Lovett (1997)
Y_{017}	5.0×10^{-8} M	McHenry and Kornberg (1977)
Y_{20}	5.0×10^{-7} M	Friedberg et al. (1995)

Table C.1
Parameters of UV mutagenesis model.

Parameter	Value	Reference
$\theta_{0,\ mutS}$	4	Hongbo et al. (2000)
$\theta_{0,\ mutL}$	3.4	Hongbo et al. (2000)
$\theta_{0,\ mutH}$	4.1	Hongbo et al. (2000)
$\theta_{0,\ umu,\ mut}$	2.7	Hongbo et al. (2000)
θ_1	10^{-9}	Drake (1969)
θ_2	3.31×10^{-2}	Keseler et al. (2011), Aksenov et al. (1997)
θ_3	2.72×10^{-9}	This paper
$\theta_{3,\ mut}$	6.95×10^{-9}	This paper
k_s	4.1×10^{-6}	This paper
$k_{s,\ mut}$	1.05×10^{-5}	This paper
m_0	50	Aksenov et al. (1997)
L_0	4,639,675 base pairs	Keseler et al. (2011)
L_1	3075	Keseler et al. (2011)

5′ (ExoVII, RecJ) exonucleases. y_{13} and y_{16} are the intermediate complexes formed by 3′ and 5′ exonucleases respectively. y_{14} represents the amount of single-stranded DNA remained after excision. y_{17} is the normalized concentration of PolIII. y_{18} describes the level of the intermediate complex representing PolIII molecules bound to a single-strand gap. y_{19} is the level of the newly synthesized DNA sequence before ligation. The last MMR stage is characterized in the model by a reaction describing the ligation of a new sequence by a DNA ligase (y_{20}), where y_{21} is the intermediate complex and y_{22} is repaired DNA.

In our model y_{01}, y_{03}, y_{05}, y_{06}, y_{09}, y_{012}, y_{015}, y_{017}, and y_{020} are the time-independent parameters representing the normalized initial levels of $MutS_2$, $MutL_2$, MutH, GATCm, UvrD, 3′ and 5′ exonucleases, PolIII, and DNA ligase, respectively. The initial concentrations of all intermediate complexes are assumed to be zero at the beginning of repair. The variables of the model are normalized per initial level of the MutS protein: $y_i = Y_i/Y_{01}$, $y_{0i} = Y_{0i}/Y_{01}$. The values of the parameters Y_{0i} are presented in Table B.1.

Kinetic parameters of the MMR model

The dimensionless parameters of Eq. (B.1) are $\tau = k_2 t$, $p_1 = k_1 Y_{01}/k_2$, $p_2 = k_2/k_2 = 1$, $p_3 = k_3/k_2$, $p_4 = k_4 Y_{01}/k_2$, $p_5 = k_5/k_2$, $p_6 = k_6 Y_{01}/k_2$, $p_7 = k_7/k_2$, $p_8 = k_8 Y_{01}/k_2$, $p_9 = X_{01}/\gamma_9$, $p_{10} = 1/(\gamma_9 N_A)$, $p_{11} = k_{11} Y_{01}/k_2$, $p_{12} = k_{12}/k_2$, $p_{13} = k_{13}/k_2$, $p_{14} = k_{14} Y_{01}/k_2$, $p_{15} = k_{15}/k_2$, $p_{16} = k_{16}/k_2$, $p_{17} = k_{17} Y_{01}/k_2$, $p_{18} = k_{18}/k_2$, $p_{19} = k_{19}/k_2$, $p_{20} = k_{20} Y_{01}/k_2$, $p_{21} = k_{21}/k_2$, $p_{22} = k_{22}/k_2$, $p_{23} = k_{23} Y_{01}/k_2$, $p_{24} = k_{24}/k_2$, $p_{25} = k_{25}/k_2$. Here t is the dimensional time; k_2 is the rate constant of the reverse reaction between $MutS_2$ and a mismatch; Y_{01} is the basal level of the $MutS_2$ protein in the cell in the absence of MMR-inducing lesions; and γ_9 is the dissociation rate constant of the LexA monomer from the *uvrD* gene operator.

The kinetic rates estimated by the fitting procedure are presented in Table B.1. Dissociation rate constant γ_9 is assumed to be equal to the average value of the LexA dissociation rate from the SOS-box (Belov et al., 2009; Mohana-Borges et al., 2000). The value of the Hill coefficient h_9 is defined from the data on the binding cooperativity of the LexA repressor and *uvrD* regulatory region. As there is the only region of LexA binding to the *uvrD* operator (Smith and Walker, 1998), h_9 equals to 2 according to Aksenov et al. (1997). The value of the parameter k_3, was set equal to α in the model of SOS network.

Appendix C. Parameters of UV mutagenesis model

See Table C.1.

References

Aksenov, S.V., 1999. Dynamics of the inducing signal for the SOS regulatory system in *Escherichia coli* after ultraviolet irradiation. Math. Biosci. 157, 269–286, http://dx.doi.org/10.1016/S0025-5564(98)10086-X.

Aksenov, S.V., Krasavin, E.A., Litvin, A.A., 1997. Mathematical model of the SOS response regulation of an excision repair deficient mutant of *Escherichia coli* after ultraviolet light irradiation. J. Theor. Biol. 186, 251–260.

Belov, O.V., 2011. Modeling base excision repair in *Escherichia coli* bacterial cells. Phys. Part. Nucl. Lett. 8, 141–148, http://dx.doi.org/10.1134/S1547477111020038.

Belov, O.V., Krasavin, E.A., Parkhomenko, A.Yu., 2009. Model of SOS-induced mutagenesis in bacteria *Escherichia coli* under ultraviolet irradiation. J. Theor. Biol. 261, 388–395, http://dx.doi.org/10.1016/j.jtbi.2009.08.016.

Bianco, P.R., Kowalczykowski, S.C., 1999. RecA protein, Encyclopedia of Life Sciences. Nature Publishing Group, London.

Borden, A., O'Grady, P.I., Vandewiele, D., Fernández de Henestrosa, A.R., Lawrence, C.W., Woodgate, R., 2002. *Escherichia coli* DNA Polymerase III can replicate efficiently past a T–T cis–syn cyclobutane dimer if DNA polymerase V and the 3′ to 5′ exonuclease proofreading function encoded by *dnaQ* are inactivated. J. Bacteriol. 184, 2674–2681.

Burckhardt, S.E., Woodgate, R., Scheuermann, R.H., Echols, H., 1988. UmuD mutagenesis protein of *Escherichia coli*: overproduction, purification and cleavage by RecA. Proc. Natl. Acad. Sci. 85, 1811–1815.

Cadet, J., Vigny, P., 1990. The photochemistry of nucleic acids. In: Morrison, H. (Ed.), Bioorganic Photochemistry. Wiley & Sons, New York, pp. 1–272.

Chiapperino, D., Cai, M., Sayer, J.M., Yagi, H., Kroth, H., Masutani, C., Hanaoka, F., Jerina, D.M., Cheh, A.M., 2005. Error-prone translesion synthesis by human DNA polymerase Z on DNA-containing deoxyadenosine adducts of 7,8-dihydroxy-9,10-epoxy-7,8,9,10-tetrahydrobenzo[a]pyrene. J. Biol. Chem. 280, 39684–-39692, http://dx.doi.org/10.1074/jbc.M508008200.

Cooper, D.L., Lahue, R.S., Modrich, P., 1993. Methyl-directed mismatch repair is bidirectional. J. Biol. Chem. 268, 11823–11829.

Courcelle, J., Khodursky, A., Peter, B., Brown, P.O., Hanawalt, P.C., 2001. Comparative gene expression profiles following UV exposure in wild-type and SOS-deficient Escherichia coli. Genetics 158, 41–64.

Drake, J.W., 1969. Spontaneous mutation: comparative rates of spontaneous mutation. Nature 221, 1132, http://dx.doi.org/10.1038/2211133a0.

Dutra, B.E., Sutera, V.A., Lovett, J.T., Lovett, S.T., 2007. RecA-independent recombination is efficient but limited by exonucleases. Proc. Natl. Acad. Sci. USA 104, 216–221, http://dx.doi.org/10.1073/pnas.0608293104.

Easton, A.M., Kushner, S.R., 1983. Transcription of the uvrD gene of Escherichia coli is controlled by the lexA repressor and by attenuation. Nucleic Acids Res. 11, 8625–8640.

Feng, G., Tsui, H.C., Winkler, M.E., 1996. Depletion of the cellular amounts of the MutS and MutH methyl-directed mismatch repair proteins in stationary-phase *Escherichia coli* K-12 cells. J. Bacteriol. 178, 2388–2396.

Friedberg, E.C., Walker, G.C., Siede, W., 1995. DNA Repair and Mutagenesis. ASM Press, Washington, D.C.

Fujii, S., Fuchs, R.P., 2004. Defining the position of the switches between replicative and bypass DNA polymerases. EMBO J. 23, 4342–4352.

Goodman, M.F., Woodgate, R., 2000. The biochemical basis and *in vivo* regulation of SOS-induced mutagenesis promoted by *Escherichia coli* DNA Polymerase V ($UmuD'_2C$). Cold Spring Harbor Symp. Quant. Biol. 65, 31–40.

Haggerty, T.J., Lovett, S.T., 1997. IF3-mediated suppression of a GUA initiation codon mutation in the recJ gene of *Escherichia coli*. J. Bacteriol. 179, 6705–6713.

Hegde, S., Sandler, S.J., Clark, A.J., Madiraju, M.V., 1995. recO and recR mutations delay induction of the SOS response in *Escherichia coli*. Mol. Genet. Genomics 246, 254–258, http://dx.doi.org/10.1007/BF00294689.

Hongbo, L., Stephen, R., Hays, H.B., Hays, J.B., 2000. Antagonism of ultraviolet-light mutagenesis by the methyl-directed mismatch-repair system of *Escherichia coli*. Genetics 154, 503–512.

Keseler, I.M., Collado-Vides, J., Santos-Zavaleta, A., Peralta-Gil, M., Gama-Castro, S., Muñiz-Rascado, L., Bonavides-Martinez, C., Paley, S., Krummenacker, M., Altman, T., Kaipa, P., Spaulding, A., Pacheco, J., Latendresse, M., Fulcher, C., Sarker, M., Shearer, A.G., Mackie, A., Paulsen, I., Gunsalus, R.P., Karp, P.D., 2011. EcoCyc: a comprehensive database of *Escherichia coli* biology. Nucleic Acids Res. 39, D583–D590, http://dx.doi.org/10.1093/nar/gkq1143.

Kornberg, A., Baker, T.A., 1992. DNA Replication. W.H. Freeman and Company, New York.

Krasavin, E.A., Kozubek, C., 1991. Mutagenic Action of Radiation With Different LET. Energoatomizdat, Moscow.

Lahue, R.S., Au, K.G., Modrich, P., 1989. DNA mismatch correction in a defined system. Science 245, 160–164, http://dx.doi.org/10.1126/science.2665076.

Li, G.M., 2008. Mechanisms and functions of DNA mismatch repair. Cell Res. 18, 85–98, http://dx.doi.org/10.1038/cr.2007.115.

Livneh, Z., 2000. DNA damage control by novel DNA polymerases: Translesion replication and mutagenesis. J. Biol. Chem. 276, 25639–25642.

Malina, J., Novakova, O., Natile, G., Brabec, V., 2012. The thermodynamics of translesion DNA synthesis past major adducts of enantiomeric analogues of antitumor cisplatin. Chem. Asian J. 7, 1026–1031, http://dx.doi.org/10.1002/asia.201100886.

Martin, L.M., Marples, B., Coffey, M., Lawler, M., Lynch, T.H., Hollywood, D., Marignol, L., 2010. DNA mismatch repair and the DNA damage response to ionizing radiation: Making sense of apparently conflicting data. Cancer Treat. Rev. 36, 518–527, http://dx.doi.org/10.1016/j.ctrv.2010.03.008.

Matson, S.W., Robertson, A.B., 2006. The UvrD helicase and its modulation by the mismatch repair protein MutL. Nucleic Acids Res. 34, 4089–4097, http://dx.doi.org/10.1093/nar/gkl450.

McHenry, C.S., Kornberg, A., 1977. DNA polymerase III holoenzyme of Escherichia coli, purification and resolution into subunits. J. Biol. Chem. 252, 6478–6484.

Modrich, P., Lahue, R., 1996. Mismatch repair in replication fidelity, genetic recombination, and cancer biology. Annu. Rev. Biochem. 65, 101–133, http://dx.doi.org/10.1146/annurev.bi.65.070196.000533.

Mohana-Borges, R., Pacheco, A.B.F., Sousa, F.J.R., Foguel, D., Almeida, D.F., Silva, J.L., 2000. LexA repressor forms stable dimers in solution. J. Biol. Chem. 275, 4708–4712.

Petit, M.A., Dervyn, E., Rose, M., Entian, K.D., McGovern, S., Ehrlich, S.D., Bruand, C., 1998. PcrA is an essential DNA helicase of *Bacillus subtilis* fulfilling functions both in repair and rolling-circle replication. Mol. Microbiol. 29, 261–273, http://dx.doi.org/10.1046/j.1365-2958.1998.00927.x.

Pham, P., Rangarajan, S., Woodgate, R., Goodman, M.F., 2001. Roles of DNA polymerases V and II in SOS-induced error-prone and error-free repair in *Escherichia coli*. Proc. Natl. Acad. Sci. 98, 8350–8354.

Pluciennik, A., Burdett, V., Lukianova, O., O'Donnell, M., Modrich, P., 2009. Involvement of the β clamp in methyl-directed mismatch repair *in vitro*. J. Biol. Chem. 284, 32782–32791.

Radman, M., 1974. Phenomenology of an inducible mutagenic DNA repair pathway in *Escherichia coli*: SOS-repair hypothesis. In: Prakash, L., Sherman, F., Miller, M., Lawrence, C., Tabor, H.W. (Eds.), Molecular and Enveronmental Aspects of Mutagenesis. Charles C Thomas Publisher, Springfield, IL, pp. 128–142.

Radman, M., Wagner, R., 1986. Mismatch repair in *Escherichia coli*. Annu. Rev. Genet. 20, 523–538, http://dx.doi.org/10.1146/annurev.ge.20.120186.002515.

Rupert, C.S., 1975. Enzymatic photoreactivation: overview. In: Hanawalt, P., Setlow, R. (Eds.), Molecular Mechanisms for Repair of DNA, Part A. Plenum Press, New York, pp. 73–87.

Rupp, W.D., Howard-Flanders, P., 1968. Discontinuities in the DNA synthesized in an excision-defective strain of *Escherichia coli* following ultraviolet irradiation. J. Mol. Biol. 31, 291–304.

Sancar, A., Sancar, G.B., 1988. DNA repair enzymes. Annu. Rev. Biochem. 57, 29–67.

Sassanfar, M., Roberts, J.W., 1990. Nature of the SOS-inducing signal in *E. coli*. The involvement of DNA replication. J. Mol. Biol. 212, 79–96.

Smith, B.T., Walker, G.C., 1998. Mutagenesis and more: *umuDC* and the *Escherichia coli* SOS response. Genetics 148, 1599–1610.

Tang, M., Pham, P., Shen, X., Taylor, J.S., O'Donnell, M., Woodgate, R., Goodman, M.F., 2000. Roles of *E. coli* DNA polymerases IV and V in lesion-targeted and untargeted SOS mutagenesis. Lett. Nat. 404, 1014–1018, http://dx.doi.org/10.1038/35010020.

Vaidyanathan, V.G., Cho, B.P., 2012. Sequence effects on translesion synthesis of an aminofluorene-DNA adduct: conformational, thermodynamic, and primer extension kinetic studies. Biochemistry 51, 1983–1995, http://dx.doi.org/10.1021/bi2017443.

Viswanathan, M., Lovett, S.T., 1999. Exonuclease X of *Escherichia coli*. A novel 3′–5′ DNase and DnaQ superfamily member involved in DNA repair. J. Biol. Chem. 274, 30094–30100, http://dx.doi.org/10.1074/jbc.274.42.30094.

Wang, S.Y., 1976. Pyrimidine bimolecular photoproducts. In: Wang, S.Y. (Ed.), Photochemistry and Photobiology of Nucleic Acids. Academic Press, New York, pp. 295–356.

Wang, Z., 2001. Translesion synthesis by the UmuC family of DNA polymerase. Mutat. Res. 486, 59–70, http://dx.doi.org/10.1016/S0921-8777(01)00089-1.

Witkin, E.M., 1976. Ultraviolet mutagenesis and inducible DNA repair in *Escherichia coli*. Bacteriol. Rev. 40, 869–907.

Woodgate, R., Rajagopalan, M., Lu, C., Echols, H., 1989. UmuC mutagenesis protein of *Escherichia coli:* purification and interaction with UmuD and UmuD′. Proc. Natl. Acad. Sci. 86, 7301–7305.

Yang, I., Miller, H., Wang, Z., Frank, E.G., Ohmori, H., Hanaoka, F., Moriya, M., 2003. Mammalian translesion DNA synthesis across an acrolein-derived deoxyguanosine adduct. J. Biol. Chem. 278, 13989–13994, http://dx.doi.org/10.1074/jbc.M212535200.